Available online at www.sciencedirect.com
ScienceDirect
Journal of Catalysis 246 (2007) 147–157
JOURNAL OF CATALYSIS
www.elsevier.com/locate/jcat

The role of autoreduction and of oxygen mobility in N_2O decomposition over Fe-ZSM-5

Gerhard D. Pirngruber *, Pijus K. Roy, R. Prins

Institute of Chemical and Bioengineering, ETH Zurich, Switzerland

Received 15 October 2006; revised 21 November 2006; accepted 29 November 2006

Available online 3 January 2007

Abstract

The mechanism of N_2O decomposition was studied on a series of Fe-ZSM-5 catalysts prepared by ion exchange (IE) and chemical vapor deposition (CVD). N_2O decomposition activity depends strongly on the extent of autoreduction of the catalyst during the pretreatment in He at high temperatures. The extent of autoreduction is significantly lower for catalysts prepared by CVD compared with that for catalysts prepared by aqueous ion exchange. As a result, the global turnover frequencies of the ion-exchanged catalysts are significantly higher. If the activity is normalized by the concentration of Fe^{2+} sites, however, then the CVD catalyst is the most active sample. This is attributed to the fact that high iron loading favors the surface migration and recombination of surface oxygen atoms to O_2, which is the rate-limiting step of the reaction. O_2 formation by slow recombination of two surface oxygen atoms is the dominating mechanism even for IE samples with very low iron loadings.

Keywords: Transient response kinetics; Isotope labeling; XANES; $^{18}O_2$; Oligonuclear iron species; Monomers; Dimers

1. Introduction

The postsynthetic introduction of iron into zeolites generates various iron species, including isolated cations, dimers, oligonuclear clusters, and large Fe_2O_3 particles. Depending on the preparation method used, one of these species may represent the majority of the iron sites; however, in most cases, mixtures of several species are present. Chemical vapor deposition (CVD) leads to a Fe/Al ratio close to 1.0 [1,2], that is, a high iron loading and strongly clustered (oligonuclear) iron species. Aqueous ion exchange (IE), if well performed, prevents the formation of clustered species and generates isolated cations or dimers. The role of the different iron species in catalytic reaction has been discussed in depth. Isolated iron cations [3] and dimers [4,5] have been suggested to be the active sites in the oxidation of benzene to phenol. Grünert and co-workers demonstrated that isolated iron species (or, in light of recent findings [6], isolated sites and/or dimers) are very active in the selective catalytic reduction of NO by isobutane or NH_3, but oligomeric species also contribute to the activity, especially in NH_3-SCR [7,8]. Perez-Ramirez et al. compared the performance of extra-framework Fe-silicalite (containing mainly isolated iron sites) and extra-framework Fe-ZSM-5 (containing mainly clustered species) in the decomposition of N_2O and concluded that the latter catalyst is more active because the clusters facilitate the recombination of two deposited oxygen atoms to O_2 [9]. For the reduction of N_2O by CO or C_3H_8, however, isolated iron sites (i.e., catalyst extra-framework Fe-silicalite) were more active. Nobukawa et al. recently confirmed the importance of having a minimum degree of aggregation of the iron species (at least dimers) for N_2O decomposition [10]. They showed that the turnover frequency of N_2O decomposition over ion-exchanged Fe-MFI catalysts increased with increasing Fe/Al ratio, and attributed this effect to the formation of iron dimers at high Fe/Al ratios. The original work of El-Malki et al. reached a similar conclusion [11]. In contrast, Heyden et al. proposed that isolated iron cations are responsible for N_2O decomposition [12,13]. They based their proposal on EXAFS measurements

* Corresponding author. Present address: Institut Français du Pétrole, Department of Catalysis and Separation, 69390 Vernaison, France. Fax: +33 4 78 02 20 66.

E-mail address: gerhard.pirngruber@ifp.fr (G.D. Pirngruber).

0021-9517/$ – see front matter
doi:10.1016/j.jcat.2006.11.030

of their samples showing that they contained mainly isolated iron cations at the ion-exchange positions [14].

The question of which iron sites are active for N_2O decomposition certainly does not have a simple answer. Isolated sites, dimers, and oligonuclear species all contribute to catalytic activity, especially at high temperatures [9]. Nonetheless, a valid question is which sites are most favorable for N_2O decomposition. To contribute to the ongoing discussion, we report a detailed comparison of two samples, Fe-ZSM-5 prepared by CVD and by IE. The former represents clustered iron species; the latter, a mixture of isolated sites and dimers [6]. We deliberately exclude from the comparison samples that were steamed or treated at very high temperatures (>1000 K), because these treatments generate qualitatively different types of sites. Our study focuses on the autoreduction and mobility of the iron species and shows the relationship between these two parameters and N_2O decomposition activity.

2. Experimental

2.1. Preparation of the Fe-ZSM-5 catalysts

The parent Na-ZSM-5 zeolites were provided by Zeochem (PZ 2-40, Si/Al = 25) and Alsi Penta (SM 27, Si/Al = 12). NH_4-ZSM-5 was obtained from Na-ZSM-5 by threefold ion exchange with a 1 M aqueous solution of NH_4NO_3 at room temperature. For the exchange with iron, 2 g of parent ZSM-5 (either Na-ZSM-5 or NH_4-ZSM-5) was suspended in 40–50 ml of H_2O. The solution was degassed with N_2 before the iron salt ($FeCl_2{\cdot}4H_2O$ or $FeSO_4{\cdot}7H_2O$) was added. Finally, the suspension was refluxed for 4–6 h at 353 K. The solid was collected by filtration, thoroughly washed, dried at 383 K, and calcined in air at 773 K for 5 h. Exchange with Fe^{2+} salts is preferred over exchange with Fe^{3+} salts, because the latter are more prone to the formation of insoluble hydroxides, which deposit on the outer surface of the zeolite. Moreover, the direct exchange of Fe^{3+} cations in ZSM-5 is difficult due to an insufficient local charge balance by the framework. During calcination, Fe^{2+} is oxidized to Fe^{3+}. The conditions of the IE, the chemical composition of the samples, and their codes are listed in Table 1.

The Fe-ZSM-5 CVD catalyst was identical to the sample used in earlier work [15]. Briefly, it was prepared by sublimation of $FeCl_3$ onto H-ZSM-5 in a flow of He at 593 K, followed by extensive washing and calcination.

2.2. Catalyst characterization

UV–vis spectra were recorded in diffuse reflectance on a Cary 400 UV–vis spectrometer using a Praying Mantis sample stage from Harrick. IR spectra of thin self-supporting pellets were measured in transmission at 473 K, after pretreatment in He at 673 K. The magnetic susceptibility was measured in the temperature range of 2–300 K in a field of 0.5 T, using a Physical Properties Measurement System (Quantum Design).

In situ XANES measurements were performed at station E4, Hasylab, Hamburg, Germany. The spectra were recorded while the catalysts were heated from 423 to 848 K in He, after an initial treatment in 3% O_2 in He at 773 K. The X-ray beam was monochromatized with two independently driven Si(111) crystals. The two crystals were detuned to 50% of the maximum reflectivity to reject higher-order reflections. The XANES spectra of the Fe K-edge were recorded in the energy range of 7.0–7.25 (or 7.40) keV. The XANES spectra of the Fe-ZSM-5 $IE_{2.8}$ catalyst were measured in transmission mode, using an in situ cell with Kapton windows, which resembles a plug-flow reactor [16]. For the catalysts with low concentration (e.g., Fe-ZSM-5 $IE_{0.4}$), the XANES spectra were recorded in fluorescence mode using a single-pixel solid-state detector. The sample was gently pressed into an Al cell body equipped with a gas inlet and a gas outlet [17]. An Al foil (99.999% purity, 20 μm thickness) sealed the sample and also served as a window for the X-rays. The cell was screwed to a heater block, which allowed the sample to be heated up to a maximum of 850 K.

2.3. Steady state N_2O decomposition

The steady-state N_2O decomposition activity was measured after pretreatment of the catalyst at 873 K in He for 1 h. A 50-mg sample of pelletized catalyst (mesh size 250–300 μm) was first treated in a flow of 10% O_2 in He at 673 K to remove adsorbed impurities, then heated to 873 K in He. Finally, the catalyst was cooled to 573 K in He, and 2500 ppm of N_2O in He was fed to the catalyst. The flow over the reactor was kept at 50 ml_{NTP}/min, corresponding to a gas hour space velocity (GHSV) of 40,000 h^{-1}. The decomposition of N_2O was followed for 30 min at each temperature before the temperature was increased at a rate of 25–50 K up to a maximum of 823 K. Gas chromatography was used to detect N_2, N_2O, and O_2. The product gases were analyzed three times at a specific temperature, and an average value was taken for evaluation of the

Table 1
Conditions of ion exchange and iron loading of the samples

Catalyst	Parent zeolite	Si/Al	Iron salt	Exchange time (h)	Fe (wt%)	Fe/Al	Exchange B-OH[a] (%)
Fe-ZSM-5 $IE_{0.1}$	NH_4-ZSM-5	25	$FeCl_2{\cdot}4H_2O$	4	0.13	0.04	5
Fe-ZSM-5 $IE_{0.4}$	NH_4-ZSM-5	25	$FeCl_2{\cdot}4H_2O$	5	0.4	0.12	10
Fe-ZSM-5 $IE_{0.9}$	Na-ZSM-5	25	$FeCl_2{\cdot}4H_2O$	6	0.9	0.26	45[b]
Fe-ZSM-5 $IE_{2.8}$	NH_4-ZSM-5	12	$FeSO_4{\cdot}7H_2O$	6	2.8	0.45	47
Fe-ZSM-5 CVD	H-ZSM-5	25	$FeCl_3$	3	4.5	1.1	50

[a] Exchange of Brønsted OH groups.
[b] The exchange degree is high compared to Fe/Al because the sample still contains Na^+ counterions.

activity data. The first-order rate constant (k), the activation energy (E_a), and the turnover frequency (TOF) were calculated from the following equations:

$$k = \frac{-\ln(1-x)F}{m_{\text{cat}}p},$$

$$E_a = \frac{\partial(\ln k)}{\partial(1/T)},$$

and

$$\text{TOF} = \frac{kp_{N_2O}}{n_{\text{Fe}}},$$

where x is the conversion, F is the total flow through the reactor, p is the total pressure, m_{cat} is the amount of the catalyst, T is the temperature, and n_{Fe} is the concentration of iron (in mol/g). The activation energy was determined between 698 and 773 K.

2.4. Step response experiments on isotopically labeled catalysts

In step response experiments on isotopically labeled catalysts, 50 mg of pelletized catalyst was first treated in a flow to 10% O_2 in He at 673 K to remove adsorbed impurities. To incorporate ^{18}O into the Fe-ZSM-5 sample, the catalyst was reduced in a mixture of 20% H_2 in He at 673 K for 1 h, which led to complete reduction to Fe^{2+}. The reduced catalyst was reoxidized at 673 K with 1% $^{18}O_2$ (93% ^{18}O, Eurisotop) in He for 30 min. The temperature was raised to 873 K (at a heating rate of 6 K/min) in $^{18}O_2$ and maintained for 5 min in $^{18}O_2$. Then the catalyst was allowed to autoreduce in He for 1 h at 873 K. Finally, the reactor was cooled to 673 K in He. To determine the concentration of labeled oxygen on the catalyst surface [18], a pulse of 1% CO in He was given. The pulse volume was 500 μl, corresponding to 0.2 μmol of CO. The amount of CO was negligible compared with the amount of iron in the sample, except for the catalyst Fe-ZSM-5 $IE_{0.1}$.

At 3 min after the CO pulse, a step to 5000 ppm N_2O in He was performed. After reaching steady state in N_2O decomposition, the feed gas was stepped down to He. Then step-up/step-down cycles in N_2O–He(t)–N_2O were carried out, with t increased in a stepwise manner from 2 to 20 min. The goal of these experiments was to measure the spontaneous desorption of O_2 from the catalyst.

In some experiments, the temperature was not raised above 673 K after the treatment in $^{18}O_2$, to deliberately avoid autoreduction of the catalyst. The reactor was simply flushed with He for 10 min before administering the CO pulse and the subsequent step to N_2O.

During the whole sequence, the gas flow rate over the reactor was maintained at 25 ml_{NTP}/min, corresponding to a GHSV of 20,000 h^{-1}. The pressure in the reactor was atmospheric. Due to the high dilution of N_2O, the reactor was perfectly isothermal during the transients. The reactor effluent was analyzed using a quadrupole mass spectrometer with mass fragments $m/e = 4$ (He), 28 (N_2 and N_2O), 32, 34, 36 (isotopes of O_2), 44, and 46 (N_2O and $N_2{}^{18}O$). He ($m/e = 4$) was used to normalize the signals. The time resolution was 3.5 s. The ion current or signal of each mass fragment was converted into a concentration using calibration factors. The transient experiments were corrected for the dead time of the system, which was ∼35 s.

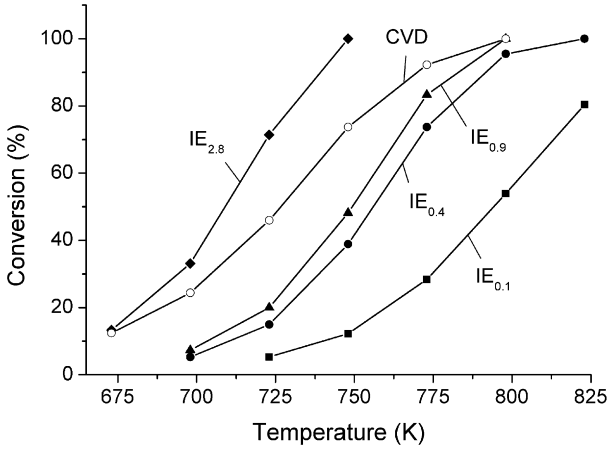

Fig. 1. Steady-state N_2O decomposition over the various catalysts after pretreatment at 873 K in He for 1 h.

Table 2
Steady-state activity of the catalysts in N_2O decomposition at 723 K after pretreatment in He at 873 K for 1 h

Catalyst	k (10^{-4} mol s^{-1} $g_{cat}{}^{-1}$ bar^{-1})	TOF (10^{-3} s^{-1})	E_a (kJ mol^{-1})
Fe-ZSM-5 $IE_{0.1}$	0.4	4.4	170
Fe-ZSM-5 $IE_{0.4}$	1.2	4.2	182
Fe-ZSM-5 $IE_{0.9}$	1.7	2.6	189
Fe-ZSM-5 $IE_{2.8}$	9.3	4.6	176
Fe-ZSM-5 CVD	4.6	1.4	129

Feed composition: 2500 ppm N_2O, balance He, GHSV = 40,000 h^{-1}.

3. Results

3.1. Steady-state N_2O decomposition

Fig. 1 shows the steady-state N_2O decomposition activity of the various catalysts after pretreatment at 873 K in He. For the catalysts prepared by IE, the activity increased gradually with increasing iron loading. The Fe-ZSM-5 CVD sample did not follow that trend. Although this sample had an iron loading of 4.5 wt%, it was less active than Fe-ZSM-5 $IE_{2.8}$. Comparing the turnover frequencies (TOFs) shows (see Table 2) that the IE samples had similar TOFs (with the exception of Fe-ZSM-5 $IE_{0.9}$), whereas the TOF of Fe-ZSM-5 CVD was significantly lower. Moreover, the conversion vs temperature curve of the CVD sample was less steep than those of the IE samples. This observation is reflected in the activation energies, which were between 170 and 190 kJ/mol for the IE samples but only 129 kJ/mol for the CVD catalyst.

These two observations indicate that the CVD and IE samples had qualitatively different behavior in N_2O decomposition. The experiments reported in the next section were designed to explain that different behavior in detail, by analyzing the type

Table 3
Effective magnetic moments (μ/β) of the catalysts and the fraction of iron monomers (p), extracted from the fits of the magnetic susceptibility curves

Catalyst	μ/β	p
Fe-ZSM-5 $IE_{0.4}$	4.6	0.64
Fe-ZSM-5 $IE_{0.9}$	3.3	0.29
Fe-ZSM-5 $IE_{2.8}$	4.3	0.48
Fe-ZSM-5 CVD	3.2	–[a]

[a] The CVD sample cannot be fitted as a mixture of monomers and dimers, due to the high fraction of oligomers.

of iron species in the samples, their autoreduction properties, and the mobility of the oxygen species.

3.2. Characterization of the samples

The IR spectra of the samples show that IE led to a reduction of the Brønsted OH band at 3605 cm^{-1}. For the IE samples, we see roughly a 1:1 correspondence between the Fe/Al ratio and the exchange degree; that is, one iron cation exchanges for one Brønsted site. For the CVD sample, this ratio was ∼2:1 (Table 1), indicating clustering of the iron species. The presence of oligonuclear iron clusters in Fe-ZSM-5 CVD and the absence of these species in all IE samples was confirmed by the UV–vis spectra (see Ref. [6]).

Magnetic measurements were used as a very sensitive probe for antiferromagnetic coupling between the iron sites, in dimers or larger clusters. The magnetic moments of all samples (Table 3) were smaller than the expected value for isolated Fe^{3+} cations of $\mu/\beta = 5.92$. To account for the reduction of the average magnetic moment, the magnetic susceptibility curves of the IE samples were fitted by a mixture of monomer and dimer terms. The fraction of monomers could be extracted from the fits, as shown in Table 3. For the Fe-ZSM-5 samples with Si/Al = 24, the fraction of monomers decreased with the Fe/Al ratio, as in the case of Cu-ZSM-5 [19]. In contrast, the fraction of monomers in Fe-ZSM-5 $IE_{2.8}$ was surprisingly high in relation to the Fe/Al ratio. The different behavior of this sample can be tentatively attributed to its lower Si/Al ratio.

The general message that we can extract from the characterization of the samples is that the IE samples represent mixtures of iron monomers and dimers, with the fraction of monomers tending to be higher in samples with low iron loading. The CVD sample contained mainly oligonuclear iron clusters (see Ref. [6] for more details).

3.3. Exchange with $^{18}O_2$

For the mechanistic studies described in the following sections, the catalysts were labeled with ^{18}O, which was incorporated by oxidation of a prereduced catalyst with $^{18}O_2$ at 673 K. Fig. 2 shows the step from He to $^{18}O_2$ (1% in He) over a reduced Fe-ZSM-5 $IE_{2.8}$ sample. The breakthrough of $^{18}O_2$ was delayed by ∼20 s. During that period, $^{18}O_2$ was entirely consumed for the oxidation of the iron sites (with about 2/3 of the iron sites oxidized within 20 s). A period of intensive exchange of $^{18}O_2$ with the catalyst followed, during

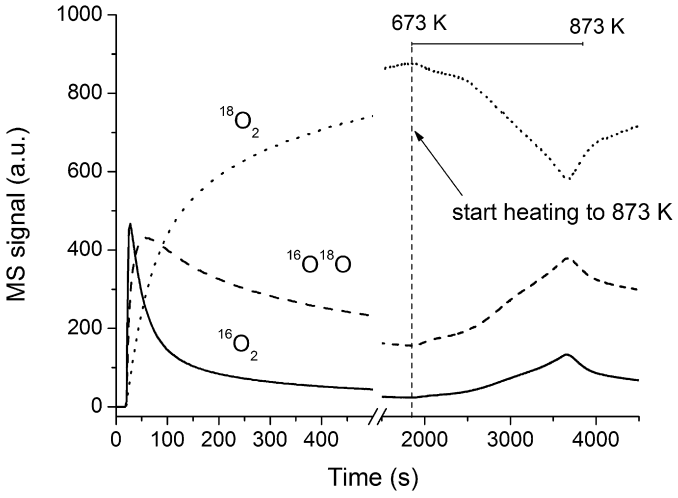

Fig. 2. Reaction of reduced Fe-ZSM-5 $IE_{2.8}$ with 1% $^{18}O_2$ in He, first at 673 K, then during heating to 873 K.

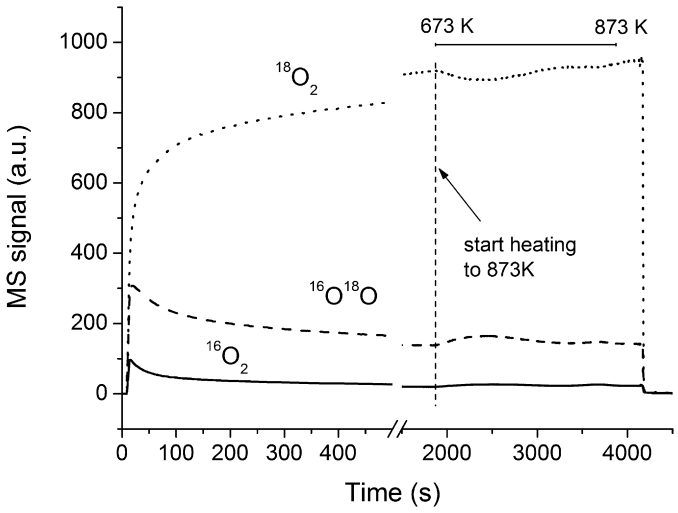

Fig. 3. Reaction of reduced Fe-ZSM-5 $IE_{0.9}$ with 1% $^{18}O_2$ in He, first at 673 K, then during heating to 873 K.

which $^{16}O_2$ and $^{16}O^{18}O$ also desorbed from the catalyst. The isotope-exchange activity gradually decreased with time on stream at 673 K; it increased again during heating to 873 K in He and reached a maximum at the endpoint of the heating ramp.

For comparison, Fig. 3 shows the reaction of reduced Fe-ZSM-5 $IE_{0.9}$ with $^{18}O_2$. After the initial reoxidation period, very little exchange of the catalyst with $^{18}O_2$ occurred, even during the heating to 873 K. The exchange activity of the other two IE catalysts was even lower, whereas Fe-ZSM-5 CVD had the greatest exchange activity of the whole series. We can conclude that the extent of isotope exchange of the catalyst with $^{18}O_2$ increased significantly with increasing iron loading.

A CO pulse was used to determine which fraction of the reactive surface oxygen atoms was ^{18}O-labeled at the end of the treatment. At 673 K, Fe-ZSM-5 readily oxidized CO to CO_2. If the isotope distribution in the product CO_2 was statistical, that

Table 4
Fraction of labeled surface oxygen atoms (^{18}f) after pretreatment of the catalysts in $^{18}O_2$ at 873 or 673 K

Catalyst	^{18}f	
	873 K	673 K
Fe-ZSM-5 $IE_{0.1}$	0.01	0.05
Fe-ZSM-5 $IE_{0.4}$	0.03	0.09
Fe-ZSM-5 $IE_{0.9}$	0.12	0.36
Fe-ZSM-5 $IE_{2.8}$	0.32	n.d.
Fe-ZSM-5 CVD	0.23	0.26

n.d. = not determined.

is, if

$$K_e = \frac{[C^{16}O^{18}O]^2}{[C^{16}O_2][C^{18}O_2]} = 4,$$

then we can assume that the fraction of labeled oxygen atoms in CO_2 was equal to the fraction of ^{18}O (^{18}f) among the surface oxygen atoms participating in CO oxidation. Unfortunately, K_e could not be calculated for the two catalysts with the lowest iron loading, because the concentration of $C^{18}O_2$ was below the detection limit of the mass spectrometer. For all of the other catalysts, K_e was 4.0 ± 0.5. Therefore, the ^{18}f of the CO_2 product provides a good measure of the concentration of labeled surface oxygen atoms. Note that the CO pulse probed only those oxygen atoms involved in CO oxidation and/or adsorption of CO_2, that is, the oxygen atoms associated with Fe. The ^{18}f values after pretreatment of the catalysts at 673 and 873 K in He are compiled in Table 4; they increased with increasing iron loading. Fe-ZSM-5 $IE_{0.1}$ and $IE_{0.4}$ contained very little labeled oxygen. The ^{18}f values were higher after pretreatment at 673 K than after pretreatment at 873 K, indicating that the ^{18}O atoms diffused away from the iron sites during He treatment at 873 K (which followed treatment in $^{18}O_2$) by exchange with oxygen atoms from the zeolite lattice. The lower the iron loading, the more pronounced the reduction of ^{18}f due to this diffusion process. The results prove that the mobility of the oxygen species at 873 K was very high and that an extensive exchange with the oxygen atoms of the zeolite framework occurred.

3.4. Transient response experiments: Step to N_2O

Fig. 4 shows the step from He to 5000 ppm of N_2O in He over the isotopically labeled Fe-ZSM-5 $IE_{0.9}$ catalyst at 673 K. The step response has the same features as described in earlier reports on Fe-ZSM-5 CVD [15,20]. A peak of N_2 can be seen immediately after the step to N_2O. The N_2 formation can be attributed to the reoxidation of Fe^{2+} sites, which were created by autoreduction, that is,

$$2Fe^{2+} + N_2O \rightarrow 2Fe^{3+} + O^{2-} + N_2. \quad (1)$$

The N_2 peak was followed by the stoichiometric decomposition of N_2O, which produced N_2 and O_2 in the expected ratio of 2. Initially, N_2O decomposition activity was very high; hereinafter, we call this period of high activity the "transient" period. Within the transient period, two N_2O decomposition

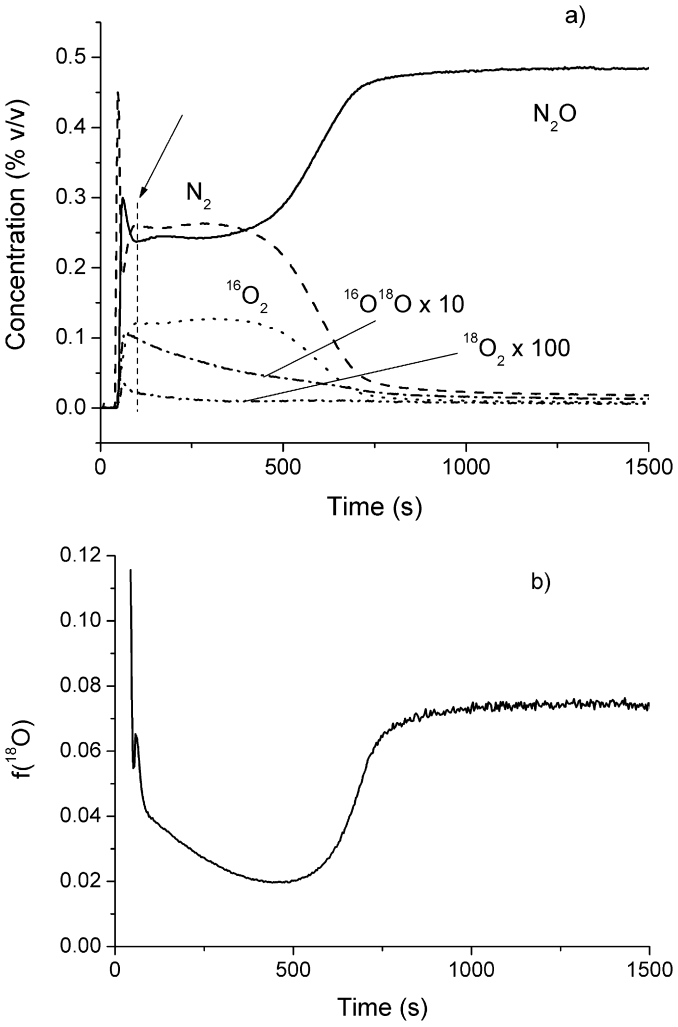

Fig. 4. Step from He to 5000 ppm N_2O in He over isotopically labeled Fe-ZSM-5 $IE_{0.9}$ at 673 K. (a) Evolution of N_2O and the reaction products with time. (b) Evolution of the fraction of labeled oxygen in the O_2 product.

processes can be discerned. The first of these processes leads to a peak of N_2 and O_2 100 s after the step to N_2O (see the arrow in Fig. 4) and is characterized by strong mixing of the isotopes in the O_2 product, with significant amounts of $^{18}O_2$ and $^{16}O^{18}O$. The labeled oxygen atoms necessarily originate from the catalyst surface and not from N_2O. The second N_2O decomposition process, which dominates the transient period and leads to the broad peak of N_2 between 150 and 500 s, incorporates only a small fraction of labeled oxygen atoms into the O_2 product (see Fig. 4b); that is, the oxygen atoms originate almost exclusively from N_2O. Once the fast, transient N_2O decomposition process is deactivated and the catalyst has reached steady state, the fraction of labeled oxygen atoms in the O_2 product increases once again. The step responses of the other IE samples were qualitatively similar to Fe-ZSM-5 $IE_{0.9}$ and are not shown. In the analysis that follows, we first focus on the behavior of the samples in steady-state N_2O decomposition; we do not discuss the transient period in detail.

We first examine the relation between steady-state activity and autoreduction. The peak of N_2 immediately after the step to N_2O (see Fig. 4) is related to the reoxidation of Fe^{2+} sites

Table 5
Results of the step-up/step-down experiments at 673 K

Catalyst	O_{dep}/Fe[a] (mol mol^{-1}) 1st step-up	TOF[b] (s^{-1}) 1st step	K_e[c]	O_{des}/Fe[d] (mol mol^{-1}) Step-down	O_{dep}/Fe[e] (mol mol^{-1}) Subsequent step-ups
Fe-ZSM-5 $IE_{0.1}$	0.3	0.0038	1.0	0.019	0.022
Fe-ZSM-5 $IE_{0.4}$	0.15	0.0037	2.2	0.009	0.012
Fe-ZSM-5 $IE_{0.9}$	0.11	0.0033	3.6	0.006	0.008
Fe-ZSM-5 $IE_{2.8}$	0.10	0.0067	3.6	0.014	0.018
Fe-ZSM-5 CVD	0.035	0.0090	3.2	0.003	0.005

[a] Amount of oxygen deposited in the first step to N_2O.
[b] Reaction rate normalized by the amount of deposited oxygen atoms in column 1.
[c] Isotope equilibrium constant of the product O_2 in steady state.
[d] Amount of oxygen atoms desorbed from the catalyst as O_2 after the step down from N_2O to He.
[e] Amount of oxygen deposited in subsequent steps from He to N_2O (average over several step-down/step-up cycles).

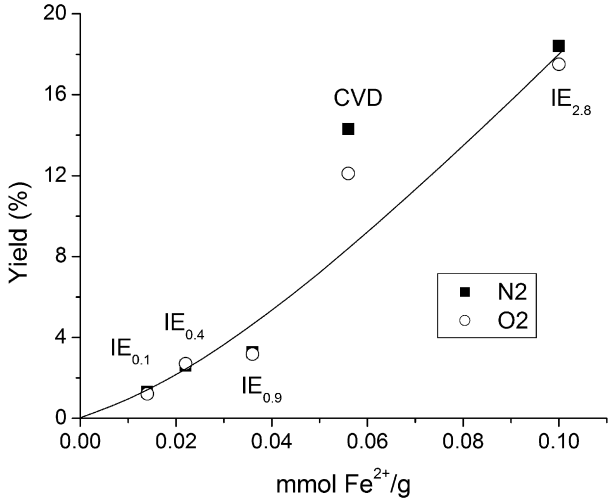

Fig. 5. Yield of N_2 and O_2 at 673 K vs the initial concentration of Fe^{2+} sites.

created by autoreduction. The concentration of Fe^{2+} can be determined by integrating the N_2 peak. The $N_2/Fe = O_{dep}/Fe$ ratios are compiled in Table 5. The O_{dep}/Fe ratio is proportional to the fraction of autoreduced sites present in the sample before the step to N_2O. According to the stoichiometry of reaction (1), the Fe^{2+}/Fe ratio is double the O_{dep}/Fe ratio. Table 5 shows that the fraction of autoreduced sites decreases with increasing iron loading of the samples. It is significantly smaller for the CVD sample than for the materials prepared by IE [21]. As reported earlier [21], the steady-state activity of the catalysts correlates well with the concentration of Fe^{2+} sites created by autoreduction at 873 K (Fig. 5). Only the CVD catalyst is significantly above the trend line of the IE samples.

The isotope distribution in the O_2 product in steady state tells us something about the origin of the oxygen atoms. A K_e value, $K_e = \frac{[^{16}O^{18}O]^2}{[^{16}O_2][^{18}O_2]}$, close to 4.0 corresponds to a statistical distribution of the isotopes in O_2 and indicates extensive exchange of the oxygen atoms on the surface before they desorb into the gas phase as O_2. The K_e value of Fe-ZSM-5 $IE_{0.1}$ is significantly lower than the statistical value. K_e increased

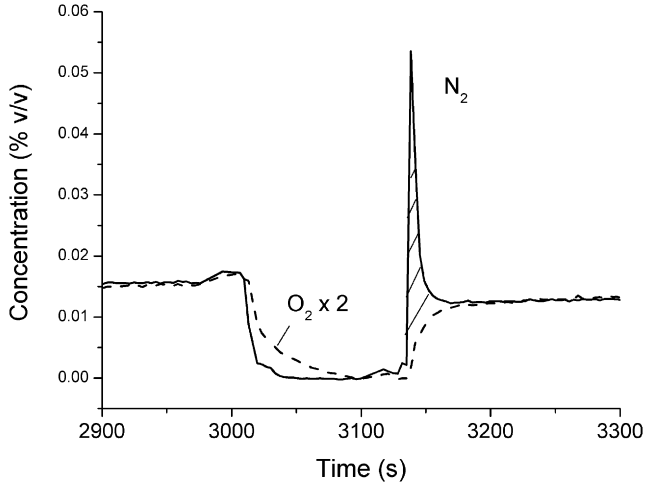

Fig. 6. Step from 5000 ppm N_2O in He to pure He, after having reached steady state in N_2O decomposition at 673 K, followed by a second step to N_2O after 2 min purge in He. The catalyst is Fe-ZSM-5 $IE_{0.9}$.

up to the 3.6 with increasing iron loading of the catalysts (Table 5).

3.5. Step-down/step-up experiments

Once the catalyst reached steady state in N_2O decomposition, the feed was switched from N_2O to pure He (step down), and then, after a short period in He (2–20 min) back to N_2O (Fig. 6). The objective of these experiments was to determine the number of active sites. The method is based on the idea that the sites participating in the catalytic cycle will release O_2 during the He purge and will then be free to be reloaded with oxygen from N_2O in the next step. Thus, their concentration can be measured by integrating the N_2 peak in the second step up. The O_{dep}/Fe ratios of the second step up, compiled in Table 5, are significantly smaller than the values of the first step to N_2O. The ratio of O_{dep} in the subsequent steps to O_{dep} in the first step is similar for all catalysts.

3.6. In situ XANES

In the step response experiments, we inferred the concentration of Fe^{2+} after autoreduction from the intensity of the initial N_2 peak. In doing so, we assumed that one N_2O reacts with two Fe^{2+} according to the stoichiometry of reaction (1). To verify this assumption, we probed the autoreduction directly using in situ XANES. The XANES spectra of Fe-ZSM-5 $IE_{2.8}$ before and after autoreduction at 848 K in He are shown in Fig. 7. Autoreduction can be seen in the shift of the Fe K-edge to lower energy and the decreased intensity of the preedge peak [22–24]. The spectrum of the fully reduced catalyst (after treatment in H_2) is included in Fig. 7 for comparison. Fitting the spectrum after autoreduction with a linear combination of the fully reduced and the fully oxidized spectrum shows that the extent of autoreduction is 32%. The edge energies at half height are 7123.1 eV (oxidized), 7121.8 eV (autoreduced), and 7119.7 eV (reduced). From the edge position, the degree of autoreduction can be interpolated as $1.3/3.4 = 38\%$, significantly

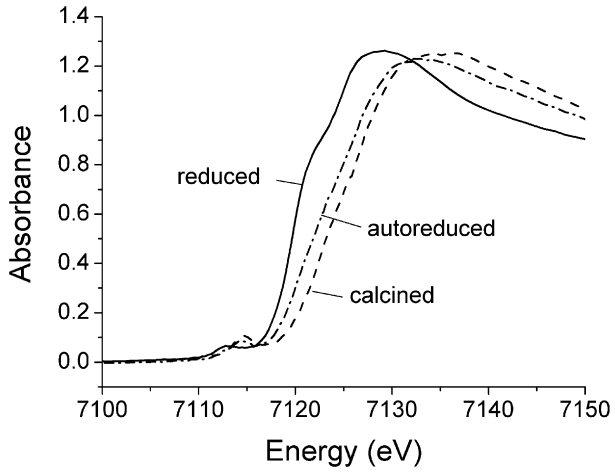

Fig. 7. XANES spectra of Fe-ZSM-5 $IE_{2.8}$ at 673 K after calcination in O_2, autoreduction in He and reduction in H_2.

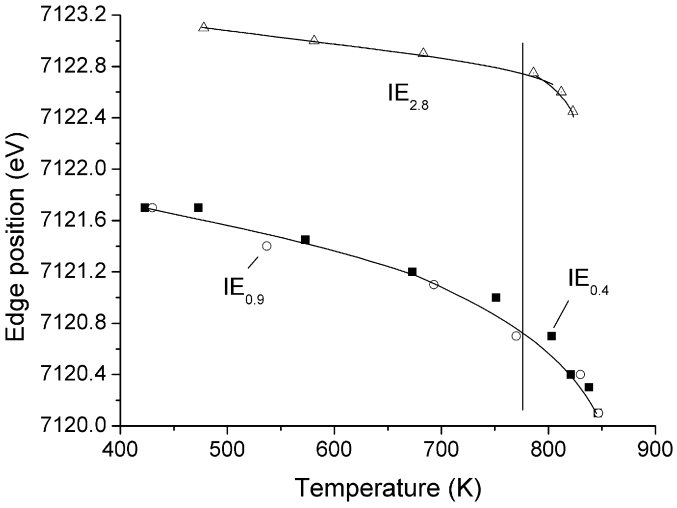

Fig. 8. Edge energy (at half height of the Fe K-edge) as a function of temperature during autoreduction of the Fe-ZSM-5 samples in He.

greater than that obtained by fitting the spectrum, indicating that the edge shift is not linearly correlated with the oxidation state. Nevertheless, the edge position at half height can be used as a qualitative measure of the oxidation state. Fig. 8 shows these positions as a function of temperature during autoreduction. Note that the absolute values of the "edge position" depend on the background subtraction. The relevant information in Fig. 8 is, therefore, not the absolute position of the edge, but rather its changes with temperature. It can be seen that very little reduction occurs up to 773 K, but that the curves become very steep above this temperature. This confirms earlier findings showing no significant autoreduction below 773 K [25]. On reaction with N_2O, the autoreduced catalysts reoxidized almost immediately to Fe^{3+}.

4. Discussion

4.1. Autoreduction of Fe-ZSM-5

Autoreduction is the spontaneous release of O_2 from the catalyst upon reduction of Fe^{3+} to Fe^{2+} [25]. The stoichiometric equation of autoreduction is

$$4Fe^{3+} + 2O^{2-} \rightarrow 4Fe^{2+} + O_2. \quad (2)$$

Equation (2) shows that the reduction of four iron atoms is required for the release of O_2. Therefore, autoreduction is certainly not a facile reaction for catalysts with low iron loadings, which contain mainly isolated iron sites at large distances from one another. It is not surprising that the release of O_2 becomes possible only at temperatures above 773 K, where, according to our isotope-exchange data, the mobility of the oxygen atoms becomes high and an extensive exchange occurs between iron-associated oxygen atoms and zeolite framework oxygen atoms. The release of O_2 should be easier on catalysts containing oligomers or clustered iron oxide species, because these can provide the four required iron atoms and/or facilitate the migration of two oxygen atoms toward each other. The experimental values show exactly the opposite trend; autoreduction increases with decreasing iron loading (Table 5). Thus, we should keep in mind that autoreduction has both a kinetic barrier and a thermodynamic barrier. Table 6 compiles the thermodynamic data for the autoreduction of bulk hematite to magnetite and FeO, that is,

$$6Fe_2O_3 \rightarrow 4Fe_3O_4 + O_2 \quad (3)$$

and

$$2Fe_2O_3 \rightarrow 4FeO + O_2. \quad (4)$$

Both reactions are strongly endothermic, and the equilibrium at room temperature is entirely on the side of Fe_2O_3. The Gibbs enthalpy of the reaction becomes negative only at temperatures above 1800 K. At 873 K (i.e., at the pretreatment temperature used in this study), the equilibrium partial pressure of O_2 is only 3×10^{-11} bar; autoreduction is thermodynamically very unfavorable and would be feasible only under ultra-high-vacuum conditions. As predicted by the thermodynamic data, catalysts containing rather large Fe_2O_3-like iron oxide clusters hardly autoreduce [26]. On the other hand, catalysts containing small iron clusters or isolated sites show considerable autoreduction already at 800–900 K. It seems that the thermodynamics of autoreduction are less unfavorable for oligomers with only a few iron atoms, particularly for isolated sites. The Madelung potential of bulk Fe_2O_3 is missing in the small clusters, and hence the high oxidation state of iron is less stable. Therefore, the IE samples, which contain only isolated sites and dimers, autoreduce more readily than the CVD samples, which contain larger oligomers. Autoreduction is controlled by thermodynamics. At the high temperature at which autoreduction becomes feasible, kinetics are no longer limiting. Because autoreduction is more pronounced for the IE catalysts, a larger fraction of the iron sites takes part in the catalytic cycle. This leads to the higher TOF of the IE catalysts reported in Table 2.

4.2. The mechanism of N_2O decomposition: IE versus CVD or isolated sites/dimers versus oligomers

In the case of Fe-ZSM-5 CVD, our earlier work provided evidence that two mechanisms of N_2O decomposition are oper-

Table 6
Thermodynamics of the autoreduction of bulk iron oxide

Reaction	ΔH_r^0 (298 K) (kJ mol^{-1})	ΔS_r^0 (298 K) (J mol^{-1})	ΔG_r^0 (298 K) (kJ mol^{-1})	T ($\Delta G_r^0 = 0$) (K)
$6Fe_2O_3 \rightarrow 4Fe_3O_4 + O_2$	482	261	404	1850
$2Fe_2O_3 \rightarrow 4FeO + O_2$	562	269	481	2090

T ($\Delta G_r^0 = 0$) $\sim \Delta H_r^0$ (298 K)/ΔS_r^0 (298 K).

ating in parallel. In the "migration–recombination" mechanism, two oxygen atoms from N_2O are deposited on two separate Fe^{2+} sites, followed by diffusion of the two oxygen atoms over the iron oxide cluster toward each other, then their recombination and desorption as O_2 [15,27]:

fast oxygen deposition:

$$2Fe^{2+} + 2N_2O \rightarrow 2[FeO]^{2+} + 2N_2 \quad (5)$$

and

$$\text{slow recombination to } O_2\text{:} \quad 2[FeO]^{2+} \rightarrow 2Fe^{2+} + O_2. \quad (6)$$

The diffusion of the oxygen atoms over the catalyst surface before desorption leads to a complete scrambling of the oxygen isotopes and K_e values close to 4.0 in the product O_2 [27]. Note that the scrambling of the isotopes occurs before the release of O_2 into the gas phase. Gas-phase O_2 does not undergo any isotope exchange under the given reaction conditions; the O_2 formation is irreversible.

In parallel to the slow O_2 desorption, which is probably controlled by surface diffusion, we also observed a rapid O_2 formation, which was (within the time resolution of our experiments, i.e., a few seconds) not delayed with respect to N_2 formation [21]. For the CVD catalyst, the contribution of this fast O_2 desorption process to the overall activity is only minor [20]. According to quantum chemical calculations [12,13], fast O_2 desorption can be attributed to the decomposition of N_2O on a single iron site. From the analysis of several possible reaction pathways, Heyden et al. deduced the following (simplified) reaction mechanism on a single iron site:

$$Z^-[FeO]^+ + N_2O\,(g) \rightarrow Z^-[FeO]^+(N_2O) \rightarrow Z^-[FeO_2]^+ + N_2\,(g), \quad (7)$$

$$Z^-[FeO_2]^+ + N_2O\,(g) \rightarrow Z^-[FeO_2]^+(N_2O) \rightarrow Z^-[OFeO_2]^+ + N_2\,(g), \quad (8)$$

$$Z^-[OFeO_2]^+ \rightarrow Z^-[FeO]^+ + O_2\,(g), \quad (9)$$

where Z^- symbolizes an ion-exchange site of the zeolite framework. The cycle involves first the formation of a peroxide species, followed by the formation of a superoxide, which then rapidly releases O_2. The first-principles calculations predict that the splitting of the second N_2O molecule [reaction (8)] to form the superoxide is rate-determining, whereas the subsequent desorption of O_2 into the gas phase is rather fast. The $[FeO]^+$ species, which stands at the beginning of the catalytic cycle, is formally a Fe^{3+} species (although its actual charge is much lower, according to a Mulliken analysis). Our results and those of others [4,28] strongly indicate that the N_2O decomposition cycle should involve Fe^{2+} species; however, we assume that a sequence similar to reactions (7)–(9) can be written for Fe^{2+} as well.

As mentioned above, the single-site mechanism seems to play only a minor role on the CVD catalyst. O_2 formation by recombination of two oxygen atoms deposited on separate sites is dominating. For the IE samples, the situation is expected to be different. These samples contain only iron monomers or dimers; thus, the recombination of two oxygen atoms deposited on two separate sites would require long diffusion paths over the zeolite matrix, which would be energetically very unfavorable. Thus, we would expect a single-site mechanism similar to the one proposed by Heyden et al. to dominate. This concept is supported by the observation that the K_e values of the Fe-ZSM-5 IE samples with low iron loadings are significantly lower than 4.0. For a reaction mechanism running on a single iron site, full scrambling of the isotopes cannot be expected.

Other experimental observations do not fit the model of Heyden et al., however. According to Heyden's calculations, O_2 desorption is fast compared with the dissociation of N_2O. (According to recent unpublished work by the same author, this holds true for iron dimers as well.) Thus, kinetic modeling predicts that O_2 formation ceases as soon as the N_2O source is interrupted (by, e.g., a step from N_2O to pure He) [13]. In contrast to these predictions, we always observe a tailing of the O_2 concentration after a step from N_2O to He (Fig. 6). Slow O_2 desorption occurs in the absence of N_2O in the feed. TAP experiments gave similar results [29–31], showing that the release of O_2 from Fe-ZSM-5 is strongly retarded and continues for a long time after pulses of N_2O are stopped. These results are not in accordance with the postulation that N_2O dissociation is rate-limiting and provide evidence supporting O_2 desorption as the rate-limiting step [32,33].

If a second step to N_2O is performed (see Fig. 6), then the initial N_2 peak corresponds to roughly twice the amount of O_2 desorbed after the step down, as expected from stoichiometry. In turn, the area of the second N_2 peak is perfectly correlated with catalytic activity (see Table 5 and Ref. [21]). Combining both of these findings leads us to conclude that N_2O decomposition activity is strongly related to the slow O_2 desorption process. This statement holds true for all of the catalysts tested in this work (i.e., both the IE and CVD samples). Because quantum chemistry convincingly predicts that O_2 desorption should not be rate-determining if two oxygen atoms from N_2O are deposited on the same iron site (monomer or dimer), our results imply that, unexpectedly, the migration–recombination mechanism also may be operative on the IE catalysts. Note, however, that others did not observe a tailing O_2 desorption after a step from N_2O to He, but rather found a rapid decay [34], as predicted by the quantum chemical calculations.

One reviewer of the present work suggested that the global kinetics (i.e., the reaction orders of N_2O and O_2) should be helpful in distinguishing the reaction mechanisms discussed above. Unfortunately, the interpretation of kinetics is not straightforward. Although O_2 formation is rate-limiting, most kinetic studies have found no or very weak inhibition of N_2O decomposition by O_2 [35,36]. O_2 formation is not limited by an adsorption–desorption equilibrium, but is limited by a recombination of two surface oxygen atoms after their migration over the surface. Therefore, at low temperatures, O_2 formation is irreversible, and O_2 does not inhibit the reaction. At high temperatures, the inhibition by O_2 increases [36] due to increasing reactivity of O_2 toward the catalyst.

The reaction order in N_2O also is not easy to explain. The experimental reaction order in N_2O is usually close to 1.0 [35,37]. Intuitively, a reaction order close to 0 would be expected if the rate were limited by the creation of oxygen vacancies. For the Fe-ZSM-5 CVD catalyst, we carried out a kinetic analysis and concluded that although O_2 formation [reaction (6)] is rate-limiting, N_2O decomposition [reaction (5)] is only two times faster at 673 K [20]. Thus, the partial pressure of N_2O affects the rate and results in an order in N_2O close to 1. At higher temperatures, the rate of O_2 formation may exceed the rate of N_2O decomposition [20,23]. The temperature at which this transition occurs will depend on the type of catalyst and may be the origin of the discrepancy between our results and those reported in Ref. [34].

4.3. Which are the most active sites for N_2O decomposition: Isolated sites, dimers, or oligomers?

In Section 4.1, we successfully related the global TOFs of the catalysts (Table 2) to the extent of autoreduction. We now can go one step further and try to determine which of the autoreduced species is the most active for N_2O decomposition. For this purpose, we calculate the TOF as the reaction rate divided by the concentration of oxygen atoms deposited on the catalyst immediately after the step to N_2O; that is, we normalize activity by the extent of autoreduction. The resulting TOFs (see Table 5) are similar for the three IE catalysts with low iron loading, but increase significantly for Fe-ZSM-5 $IE_{2.8}$ and especially for Fe-ZSM-5 CVD. At high iron loadings, the activity per Fe^{2+} site increases. This indicates that oligomeric clusters can play a beneficial role in N_2O decomposition by facilitating the surface diffusion of the deposited oxygen species. A similar conclusion was reached earlier by Perez-Ramirez et al. [9].

Within the precision of our measurements, we did not observe a difference in the TOF of Fe-ZSM-5 $IE_{0.1}$, $IE_{0.4}$, and $IE_{0.9}$ although physicochemical characterization indicated an increasing fraction of iron dimers with iron loading in that series. Thus, we conclude that isolated sites and dimers behave similarly in N_2O decomposition. This conclusion is at variance with the findings of Nobukawa et al. [10], who in a series of Fe-MFI catalysts observed increasing TOF with increasing Fe/Al ratio and attributed this to the formation of dimers. Note, however, that we also found a significantly higher TOF for Fe-ZSM-5 $IE_{2.8}$, but attribute this effect to the higher density of iron in the sample, which facilitates O_2 formation by migration/recombination, rather than to the formation of dimers (see Table 3).

4.4. The peak of N_2 after the step to N_2O

In previous sections, we used the peak of N_2 right after the step to N_2O to quantify the extent of autoreduction and calculate TOFs. We need to ensure that the peak was interpreted correctly by associating it with reaction (1). Different views have been expressed in the literature. According to the kinetic model of Heyden et al., the peak is due to reaction (7), that is, the rapid transformation of an iron-oxo species into a peroxide. The formal oxidation state of both iron species is +III; that is, oxidation of iron is not involved. Our XANES data, which show a clear oxidation of Fe^{2+} to Fe^{3+} after a step to N_2O, allow us to rule out that option.

There is also a debate about the stoichiometry of oxidation of Fe^{2+} by N_2O. Normally, one N_2O molecule can oxidize two iron atoms. Yet, it was argued that the reaction

$$2Fe^{2+} + N_2O \rightarrow Fe^{3+}\text{–}O^{2-}\text{–}Fe^{3+} + N_2 \quad (1a)$$

would lead to a rather unreactive O^{2-} species. In that case, we would have difficulty explaining the high reactivity of the deposited oxygen atoms. Therefore, it was proposed [4,24] that N_2O should react according to

$$Fe^{2+} + N_2O \rightarrow Fe^{3+}\text{–}O^{\bullet -} + N_2. \quad (10)$$

This reaction leads to a highly reactive radical anion and naturally explains the high reactivity of N_2O on Fe-ZSM-5. On samples treated under harsh conditions at very high temperatures, a 1:1 stoichiometry between Fe^{2+} and N_2O indeed has been observed [4,5,38,39]. However, the XANES data for the samples used in the present work speak against a 1:1 stoichiometry of the oxidation of Fe^{2+} by N_2O. These data indicate that the 2:1 stoichiometry of reaction (1) is valid. How can we reconcile the validity of reaction (1) with the earlier statement that reaction (1) formally generates nonreactive O^{2-} species? At the moment, we are not able to identify the precise nature of the deposited oxygen atom. All we can say is that, although the stoichiometry of reaction (1) is respected, the deposited oxygen atom is more reactive than a conventional O^{2-} lattice anion.

5. Conclusion

The N_2O decomposition activity of Fe-ZSM-5 catalysts is strongly correlated with the autoreduction of the iron sites. The extent of autoreduction decreases in the order monomers, dimers > oligomers > Fe_2O_3 particles. The reason for this sequence is the thermodynamic stability of Fe^{2+} compared with Fe^{3+}, which decreases in the same order. Consequently, the global TOFs of the IE samples, which contain mainly isolated sites or dimers, are higher than those of the CVD catalysts, which contain mainly oligomeric iron species. If we normalize the catalytic activity by the extent of autoreduction, the picture looks different. The activity per Fe^{2+} site increases significantly at high iron loadings, because the recombination of O_2 via the

migration of two surface oxygen atoms is favored. The highest activity per Fe^{2+} site is observed for the CVD sample, which contains oligonuclear iron species.

The optimal iron loading of a sample depends on the trade-off between the increased TOF (per Fe^{2+} site) and the decreased autoreduction. Increasing the iron loading is favorable, as long as the formation of oligonuclear iron species and larger clusters can be avoided. The latter do not autoreduce easily, and the fraction of iron sites taking part in the catalytic cycle decreases. Fe-ZSM-5 $IE_{2.8}$ is an example of an "ideal" sample for N_2O decomposition because it contains a high concentration of iron sites, all present in the form of monomers or dimers.

Concerning the mechanism of N_2O decomposition, we considered two possibilities: (i) a single-site mechanism in which N_2O deposits two oxygen atoms on the same iron site, followed by rapid O_2 desorption, and (ii) the "migration–recombination" mechanism, in which two oxygen atoms are deposited on separate iron sites, followed by a slow surface migration and recombination to O_2. Our results indicate that the latter mechanism dominates even on IE catalysts with very low iron loadings. Therefore, the mobility of the surface oxygen species is a crucial factor in determining catalyst activity.

Acknowledgments

We thank Dr. Andreas Heyden for engaging in a fruitful exchange of ideas concerning the comparison of his and our results and, in particular, for providing unpublished data. We also thank Dr. J.A.Z. Pieterse (ECN Petten) for providing the Fe-ZSM-5 $IE_{2.8}$ sample, and Drs. Konstantin Klementiev (Hasylab), Shiva Narayanappa, and Vendula Gabova (ETH Zurich) for assisting with the EXAFS measurements. DESY and the EU Commission provided beamtime and travel support under Contract RII3-CT-2004-506008. The project was financially supported by the Swiss National Science Foundation.

Appendix A

In this appendix, we briefly comment the difference between the amount of N_2 evolved in the first step to N_2O and the subsequent steps (see columns 1 and 5 of Table 5). In earlier work on CVD samples [20], we proposed the following explanation. Fe^{2+} dimers are irreversibly oxidized by N_2O according to reaction (1a). Because the oxygen atom is incorporated as an unreactive O^{2-} anion, it does not play any further role in the catalytic cycle. Only those Fe^{2+} sites that form radical anions according to reaction (10) are active and generate the N_2 peak in subsequent step-ups. In other words, we attributed the first N_2 peak mainly to reaction (1a), which is irreversible, and attributed the subsequent N_2 peaks to reaction (10). We implied that reaction (1a) would take place on Fe^{2+} dimers and reaction (10) on isolated Fe^{2+} sites (isolated in the sense that they are neighbors with another Fe^{2+} site).

The current results force us to revise that view. The ratio of N_2 produced in the first step and in the subsequent steps to N_2O was similar for all samples, even for those containing mainly isolated iron sites. Therefore, the monomer/dimer argument cannot explain the difference between the first and subsequent N_2 peaks. Instead, we prefer the following, very simple explanation: The fraction of autoreduced Fe^{2+} sites, as measured by the first N_2 peak, correctly represents the fraction of active sites. After a step down from N_2O to He, not all of these sites are able to desorb O_2, and thus all subsequent N_2 peaks are smaller.

References

[1] H.Y. Chen, W.M.H. Sachtler, Catal. Lett. 50 (1998) 125.
[2] H.Y. Chen, W.M.H. Sachtler, Catal. Today 42 (1998) 73.
[3] J. Jia, K.S. Pillai, W.M.H. Sachtler, J. Catal. 221 (2004) 119.
[4] K.A. Dubkov, N.S. Ovanesyan, A.A. Shteinman, E.V. Starokon, G.I. Panov, J. Catal. 207 (2002) 341.
[5] L. Kiwi-Minsker, D.A. Bulushev, A. Renken, J. Catal. 219 (2003) 273.
[6] G.D. Pirngruber, P.K. Roy, R. Prins, Phys. Chem. Chem. Phys. 8 (2006) 3939.
[7] M.S. Kumar, M. Schwidder, W. Grünert, U. Bentrup, A. Brückner, J. Catal. 239 (2006) 173.
[8] M. Schwidder, M.S. Kumar, A. Brückner, W. Grünert, Chem. Commun. (2005) 805.
[9] J. Perez-Ramirez, F. Kapteijn, A. Brückner, J. Catal. 218 (2003) 234.
[10] T. Nobukawa, M. Yoshida, K. Okumura, K. Tomishige, K. Kunimori, J. Catal. 229 (2005) 374.
[11] E.M. El-Malki, R.A. van Santen, W.M.H. Sachtler, J. Catal. 196 (2000) 212.
[12] A. Heyden, B. Peters, A.T. Bell, F.J. Keil, J. Phys. Chem. 109 (2005) 1857.
[13] A. Heyden, A.T. Bell, F.J. Keil, J. Catal. 233 (2005) 26.
[14] S.H. Choi, B.R. Wood, J.A. Ryder, A.T. Bell, J. Phys. Chem. B 107 (2003) 11843.
[15] P.K. Roy, G.D. Pirngruber, J. Catal. 227 (2004) 164.
[16] G.D. Pirngruber, P.K. Roy, N. Weiher, J. Phys. Chem. B 108 (2004) 13746.
[17] N. Weiher, E. Bus, B. Gorzolnik, M. Moller, R. Prins, J.A. van Bokhoven, J. Synchrot. Radiat. 12 (2005) 675.
[18] S. Tanaka, K. Yuzaki, S. Ito, S. Kameoka, K. Kunimori, J. Catal. 200 (2001) 203.
[19] P. Da Costa, B. Moden, G.D. Meitzner, D.K. Lee, E. Iglesia, Phys. Chem. Chem. Phys. 4 (2002) 4590.
[20] G.D. Pirngruber, P.K. Roy, Catal. Today 110 (2005) 199.
[21] G.D. Pirngruber, M. Luechinger, P.K. Roy, A. Cecchetto, P. Smirniotis, J. Catal. 224 (2004) 429.
[22] G. Berlier, G. Spoto, S. Bordiga, G. Ricchiardi, P. Fisicaro, A. Zecchina, I. Rossetti, E. Selli, L. Forni, E. Giamello, C. Lamberti, J. Catal. 208 (2002) 64.
[23] G. Berlier, G. Spoto, P. Fisicaro, S. Bordiga, A. Zecchina, E. Giamello, C. Lamberti, Microchem. J. 71 (2002) 101.
[24] A.A. Battiston, J.H. Bitter, W.M. Heijboer, F.M.F. de Groot, D.C. Koningsberger, J. Catal. 215 (2003) 279.
[25] T.V. Voskoboinikov, H.Y. Chen, W.M.H. Sachtler, Appl. Catal. B 19 (1998) 279.
[26] G.D. Pirngruber, L. Frunz, J.A.Z. Pieterse, J. Catal. 243 (2006) 340.
[27] G.D. Pirngruber, P.K. Roy, Catal. Lett. 93 (2004) 75.
[28] Q. Zhu, R.M. van Teeffelen, R.A. van Santen, E.J.M. Hensen, J. Catal. 221 (2004) 575.
[29] G. Mul, J. Perez-Ramirez, F. Kapteijn, J.A. Moulijn, Catal. Lett. 77 (2001) 7.
[30] J. Perez-Ramirez, F. Kapteijn, G. Mul, J.A. Moulijn, J. Catal. 208 (2002) 211.

[31] J.C. Groen, A. Brückner, E. Berrier, L. Maldonado, J.A. Moulijn, J. Perez-Ramirez, J. Catal. 243 (2006) 212.
[32] D.A. Bulushev, L. Kiwi-Minsker, A. Renken, J. Catal. 222 (2004) 389.
[33] B.R. Wood, J.A. Reimer, A.T. Bell, M.T. Janicke, K.C. Ott, J. Catal. 224 (2004) 148.
[34] K. Sun, H. Xia, E. Hensen, R. van Santen, C. Li, J. Catal. 238 (2006) 186.
[35] J. Leglise, J.O. Petunchi, W.K. Hall, J. Catal. 86 (1984) 392.
[36] F. Kapteijn, G. Marban, J. Rodriguez-Mirasol, J.A. Moulijn, J. Catal. 167 (1997) 256.
[37] C.M. Fu, V.N. Korchak, W.K. Hall, J. Catal. 68 (1981) 166.
[38] I. Yuranov, D.A. Bulushev, A. Renken, L. Kiwi-Minsker, J. Catal. 227 (2004) 138.
[39] P.K. Roy, Ph.D. thesis, ETH Zurich, 2006, http://e-collection.ethbib.ethz.ch/show?type=diss&nr=16473.